Histol Histopathol (2012) 27: 919-930
DOI: 10.14670/HH-27.919

http://www.hh.um.es

Histology and Histopathology
Cellular and Molecular Biology

Angiotensin AT_1 receptor inhibition-induced apoptosis by RhoA GTPase activation and pERK1/2 signaling pathways in neonatal obstructive nephropathy

Victoria Bocanegra[2], Martin Rinaldi Tosi[1], Andrea Gil Lorenzo[2], Valeria Cacciamani[1], Walter Manucha[1,2], Miguel Fornés[1,2] and Patricia G. Vallés[1,2]

[1]Pathophysiology Area-Pathology Department- School of Medicine- Cuyo University and
[2]MBECU-CONICET (National Council of Scientific and Technical Research of Argentina)

Summary. Intrarenal renin-Angiotensin system (RAS) activity is increased during early development and is further enhanced by unilateral ureteral obstruction (UUO).

We studied the involvement of mitogen-activated protein (MAP) kinase members and the RhoA GTPase signaling pathways on the regulation of renal cell response after AT_1 Angiotensin II receptor inhibition in obstruction.

Neonatal rats subjected to sham operation or complete UUO within the first 48 hours of life received saline vehicle, Losartan (AT_1 inhibitor), or PD-123319 (AT_2 inhibitor) during the first 14 days of life. Cortex tubular epithelial cell apoptotic response was shown by TUNEL and confirmed by electron microscopy associated with mitochondrial signaling pathway through the increased proapoptotic ratio Bax/BcL-2, and consequently increased caspase 3 expression and activity in obstructed kidney before and after Type 1 (AT_1) receptor blockade. Non injury of contralateral kidney was shown.

The convergence of two independent signal pathways, the RhoA GTPase and pERK and concurrent inhibition of JNK MAP kinase, were required for the apoptotic response in 14 day kidney obstructed tubular cells either with or without Losartan treatment. Absence of increased AT_2 protein expression after AT_1 receptor inhibition on day 14 of obstruction was shown. Selective AngiotensinAT_2-receptor inhibition with PD-123319 had no protective effect on the renal response to complete 14 day UUO.

We suggest a role of both RhoA GTPase activation and the opposing actions of the ERK and JNK-MAP kinase signaling pathways as events involved in tubular cell apoptosis regulation in neonatal UUO. The selective AT_1-receptor inhibition had no effect on the renal cellular response in the kidney subjected to UUO for 14 days.

Key words: Apoptosis. Angiotensin AT_1 receptor. RhoA. MAPKinase. UUO

Offprint requests to: Dr. Patricia G. Vallés, Área de Fisiología Patológica, Departamento de Patología, Facultad de Ciencias Médicas, Universidad Nacional de Cuyo, Centro Universitario. CP: 5500, Mendoza. Argentina. e-mail: pvalles@fcm.uncu.edu.ar

Introduction

Renal insufficiency as a result of congenital obstructive nephropathy is a consequence of impaired renal growth and maturation (Kohaut and Tejani, 1992; Peters, 1995). Renal cell proliferation is decreased, while apoptosis is increased in the developing obstructed kidney (Chevalier, 1996) leading to tubular atrophy, an end result of chronic UUO in the neonatal rat (Chevalier, 1996). The signaling pathways that lead to apoptosis are beginning to be defined, and a number of proteins have been identified that induced the apoptotic response.

Tubular stretching resulting in an axial strain with a positive relationship to apoptosis on tubular cell may be produced by UUO through a mechanical signal (Cachat et al., 2003).This mechanical signal propagates from the extracellular matrix and converges on cell surface adhesion receptors called integrins, which connect intracellularly to the actin cytoskeleton within focal adhesion units (Alenghat and Inger, 2002). Force-induced assembly of focal adhesions is mediated by activation of Rho and its downstream targets (Riveline et al., 2001; Galbraith et al., 2002). Rho proteins are a branch of GTPases that belong to the Ras superfamily,

which are critical elements of signal transduction pathways leading to a variety of cellular responses (Hall, 1998). In this way, it has been demonstrated that Rho proteins have an important role in the regulation of the apoptotic response to stress-inducing agents in different cell systems such as murine NIH3T3 fibroblasts (Esteve et al., 1998). Moreover, in renal proximal tubule epithelial cells involvement of RhoA on enhanced enzymatic activity of caspase-3 with increased percentage of apoptotic cells, has been shown after downregulation of Rnd3, an inhibitor of Rho protein function (Ionin et al., 2008).

Extracellular signal-regulated kinases (ERK1 and ERK2) have also been implicated in apoptosis induction through the regulation of transcription factors and direct phosphorylation of some proteins (Tian et al., 2000). Cyclic stretching of rabbit proximal tubular cells caused a time- and intensity-dependence activation of extracellular signal-regulated kinases 1 and 2 (ERK1/2) in proximal tubular cells (Alexander et al., 2004). Nevertheless, mitogen-activated protein (MAP) kinase family members, including JNK (c-JUN NH2-terminal protein kinase) and p38 and its´ dependent on the activation of caspase-3 and -9, have been involved on the apoptotic response of kidney-52E cells, a rat renal proximal tubular cell line (Nguyen et al., 2006).

Recent accumulating evidence highlighted the significance of these small G proteins as essential molecular switches that trigger the signal transduction and functions of Angiotensin II (Ohtsu et al., 2006), In addition, Angiotensin II- induced activation of the MAPK superfamily in kidney epithelial cells. This is of relevance since the neonatal kidney responds to UUO by marked activation of the Renin-Angiotensin system (RAS).

RAS has been shown to play an important role in the progression of interstitial fibrosis of the obstructed kidney that's why Angiotensin II inhibition in this setting would seem to be particularly important (Chevalier and Cachat, 2001). Regarding this, two recent studies have demonstrated that Angiotensin-converting enzyme inhibition or Angiotensin AT_1-receptor blockade protect the neonatally obstructed kidney against development of obstructive nephropathy (Beharrie et al., 2004; Topcu et al., 2007). However, interference with the RAS in the developing kidney leads to a broad spectrum of renal maldevelopment (Guron and Friberg, 2000). Recently, it has been demonstrated that the administration of enalapril or an AT_1 receptor antagonist during nephrogenesis exacerbates injury to the obstructed kidney (Chen et al., 2007; Coleman et al., 2007).

In order to investigate the molecular mechanisms that regulate tubular cell apoptosis in obstruction, we examined the contributions to cell death of both, the mitogen-activated protein (MAP) kinase family members, including ERK (extracellular signal-regulated kinase), JNK (c-JUN NH2-terminal protein kinase), and p38 and the Rho pathway before and after Angiotensin AT_1 receptor inhibition.

The rationale for studying the cellular response - signaling pathways in the UUO developing kidney after Angiotensin II AT_1 receptor inhibition relates to our hypothesis of persistent tubular cell apoptosis with absence of a cytoprotective effect.

Material and methods

Surgical procedure

Neonatal rats were subjected to sham operation or complete UUO within the first 48 hours of life and returned to their mothers. Control and UUO neonatal rat groups received daily normal saline, the AT_1-receptor inhibitor Losartan (Merck, Rahway, NJ), or the AT_2-receptor inhibitor, PD-123319 (Sigma-Aldrich, St. Louis, MO) on days 1 to 14 of life. Losartan and PD-123319 were given by gastric gavage, both at a dose of 10 $mg \cdot kg^{-1} \cdot day^{-1}$. Our laboratory has previously shown that this dose of Losartan prevents interstitial fibrogenesis independently of its effects on blood pressure, involving NOS isoforms and COX-2 in unilateral obstructive nephropathy (Manucha et al., 2004), while Chevalier et al showed that this dose of PD-123319 blocked Angiotensin-dependent stimulation of renal clusterin expression (Yoo et al., 2000). All the experimental procedures of this study were previously approved by the Laboratory Animal Ethical Committee of the School of Medicine, Cuyo University, Mendoza (32/95 C.D.) The experiments were conducted in accordance with guidelines of the CEEA (Ethical Committee of Animal Experimentation of Argentina.

Identification of cellular apoptosis. TUNEL technique

At harvest, each animal was weighed and anesthetized (intraperitoneal) with pentobarbital sodium. Kidneys were removed to ice-cold saline and then decapsulated before weighing. The kidneys were then fixed in 10% phosphate-buffered formalin at RT for 24 h, after which time they were dehydrated through ethanol and embedded in paraffin. For each animal, both right- and left-side kidneys were embedded together, so that staining in both could be compared directly and micrometer sections of blocks were prepared for identification of cellular apoptosis. After the digesting and quenching steps, equilibration buffer was applied directly to the sections and working strength TdT enzyme was then applied directly. A biotin-conjugated anti-digoxigenin antibody (Sigma) was used. Then, the sections were incubated with biotinylated anti-mouse IgG (Dako, Carpinteria, CA, USA) at 1:100 dilution for 45 min at RT and later with peroxidase-labeled streptavidin (strept AB Complex/HRP, Dako) at 1:100 dilution for 45 min at RT. After a brief wash, 3, 3'-diaminobenzidine tetrahydrochloride (0.5 mg/ml)/H_2O_2 (0.01%), a chromogen substrate, was incorporated. For positive control, sections from involution prostates were

used (n: 2). For the quantification of apoptotic epithelial cells in cross sectioned cortex areas, ten consecutive fields were randomly selected and were evaluated at 400x, on a 10x10 grid, using an image analyzer(Image Pro-Plus 4.0, 1998, Maryland USA).

Results were expressed as the number of apoptotic cells per mm^2.

Transmission electron microscopy

Small blocks (5 mm^3) of renal cortex tissue were immersed in the fixative solution (glutaraldehyde 4% in paraformaldehide/picric acid) for 24 hours. Fixed renal cortex tissue was rinsed twice in 20 mL of PBS and was then re-fixed in 1% OsO_4 (w/v) overnight and dehydrated through ethanol-acetone (up to absolute acetone, Merck®) and embedded in Epon 812 (Pelco, USA). Ultrathin sections were obtained in an Ultracut, (Leica ultramicrotome) and stained with uranyl acetate and lead citrate. Observations and micrographs were performed and observed in a Zeiss 900 electron microscope.

Western blot analysis

Tissue Preparation

The isolated cortexes were placed in ice-cold isolation buffer containing 300 mmol/ L sucrose, 18 mmol/L Tris HCl, 5 mmol/L sodium ethylene-glycol-tetraacetic acid (Na^+ EGTA), 4 μg/mL aprotinin, 4 μg/mL leupeptin, 2 μg/mL chymostatin, 2 μg/mL pepstatin, and 100 μg/mL 4-2 aminoethyl-benzenesulfonyl fluoride (AEBSF), pH 7.4 and were homogenized by using a Dounce style tissue homogenizer. The homogenate was centrifuged at 7000 rpm 15' at 5°C to remove incompletely homogenized fragments and nuclei. The supernatant was re-centrifuged at 19500 rpm 45' at 5°C to produce a pellet containing enriched membrane fractions and the supernatant as cytosol. The pellets were re-suspended in isolation buffer and the aliquots from total, membrane and cytosolic fractions were saved at -70°C. Protein concentrations from cortex were quantified by Lowry assay using BSA as a standard. A total of 30 μg of proteins from cortex fractions were electrophoresed in polyacrylamide minigels (Bio-Rad Mini Protean II) and subjected to blotting. After transferring to nitrocellulose membranes by electroelution, specific binding sites were blocked with 5% milk in 80 mmol/L Na_2HPO_4, 20 mmol/L NaH_2PO_4, 100 mmol/L NaCl, and 0.1% Tween 20, pH 7.5, for 1 h at room temperature, washed and then incubated with Caspase 3 (1: 500), Pro-Caspase-3 p32 goat polyclonal IgG (1:500) (Santa Cruz Biotechnology, USA), Bax (1:1000), BcL-2 (1:1000), AT_1 (1:500) and AT_2 receptors (1:2000), p38MAPK (1:500), phospho-38 MAPK (detecting p38 MAPK phosphorylated at Thr180 and Tyr182), (1:500) p-JNK (detecting phosphorilated JNK1, JNK2 and JNK3), JNK (detecting all: JNK1, JNK2 and JNK3), ERK1/2, phospho-ERK1/2 (1:500) (detecting ERK1/2 phosphorylated at Thr202 and Tyr204) (Sigma) overnight at 4°C. Rho A activation was determined by measuring membrane-bound Rho A (GTP-RhoA) using rabbit anti-Rho A antibody (1:200), Santa Cruz Biotechnology, Santa Cruz, CA. Each membrane was reprobed with alpha-tubulin as a control for the same protein loading. Detection was accomplished with secondary antibodies (DAKO) and detected with enhanced chemiluminescence system (ECL, Amersham). The chemiluminescence was detected with a FUJIFILM LAS-4000 image analyzer. Densitometric analysis was performed using the US National Institute of Health Image 1.66 software (Rasband Wayner et al, Division of computer Research and Technology NIH, Bethesda, USA).The magnitude of the immunosignal was given as a percentage of control renal tissue.

Caspase 3 activity assay

The activity of caspase 3 was determined using the CaspACETM Assay System (Promega, Madison, WI, USA). In this assay the CPP32-like proteases showed specificity for cleavage at the C-terminal side of the aspartate residue of the sequence DEVD (Asp- Glu.Val-Asp). Aliquots of cytosol homogenates were diluted in caspase assay buffer + DMSO 2 μl + DTT 100 mM 10 μl, and incubated for 30 min at 37°C. After the addition of 2.5 mM of the substrate, incubation was performed for 60 minutes at 37°C. Peptide cleavage was measured over 1 hour at RT using an spectrofluorometric fluorecent plate reader (Fluoro Count TM; AF10001, Cambers Company, USA) at a wavelength of 360 nm excitation and 460 nm emission. Specific caspase 3 activity was expressed as pmol of AMC liberated / minute /μg protein.

Statistical analysis

The results were assessed by one-way analysis of variance for comparisons among groups. Differences among groups were determined by Bonferroni post- test. $p<0.05$ was considered to be significant. Results are given as means ± SEM. Statistical tests were performed using GraphPad In Sat version 5.00 for Windows XP (Graph Pad Software, Inc, San Diego, CA, USA).

Results

Kidney weight/ body weight ratio

As shown in Table 1, decreased kidney weight/body weight ratio from the animals following 14 days of obstruction (O-H_2O) was demonstrated when it was compared to the control group (C-H_2O) and to the contralateral kidneys of the same group (CLH_2O). After administration of Losartan there were no differences in kidney weight/body weight ratio between the obstructed

kidneys from Losartan-treated rats (O-Los) to the group of neonatal obstructed kidney rats without treatment (O-H_2O). Absence of differences was shown in obstructed kidneys from Losartan compared to obstructed kidneys from PD-123319 treated rats.

Angiotensin II AT_1 and AT_2 receptor expression in obstruction. Effect of Losartan

In our study, to document Angiotensin II AT_1 receptor inhibition, expression of the receptor at the protein level was analyzed in membrane cortex kidney sections and in total cortex fractions. The AT_1 receptor protein expression was not found following Losartan treatment in the membrane cortex kidney sections from obstructed and control groups (Fig. 1A).Western blot studies in total cortex kidney fractions showed no

Table 1. Kidney weight/Body weight (g/g) in obstructed, contralateral and control rats.

	Vehicule	Losartan
Control KW/BW ratio	5.83±0.36	5.66±0.74
Obstructed KW/BW ratio	$3.49\pm0.15_{\dagger\dagger\dagger}{}^{***}$	$3.95\pm0.38_{\dagger\dagger\dagger}{}^{***}$
Contralateral KW/BW ratio	6.62±0.81	6.38±0.93

After fourteen days of obstruction, ratio of obstructed kidney weight/ body weight (OKW/BW) g/g, contralateral kidney weight / body weight ratio (CLKW/BW) g/g, and control kidney weight/body weight ratio (CKW/BW) g/g are shown. Values are means ± SEM n: 10. a: OKW/BW vs CKW/BW following 14 days of obstruction without and with Losartan treatment, ***p<0.001, both; b: OKW/BW vs CLKW/BW following 14 days of obstruction without and with Losartan treatment, †††<0.001, both. Data are mean ± S.E.M. of 3 independent experiments for each condition.

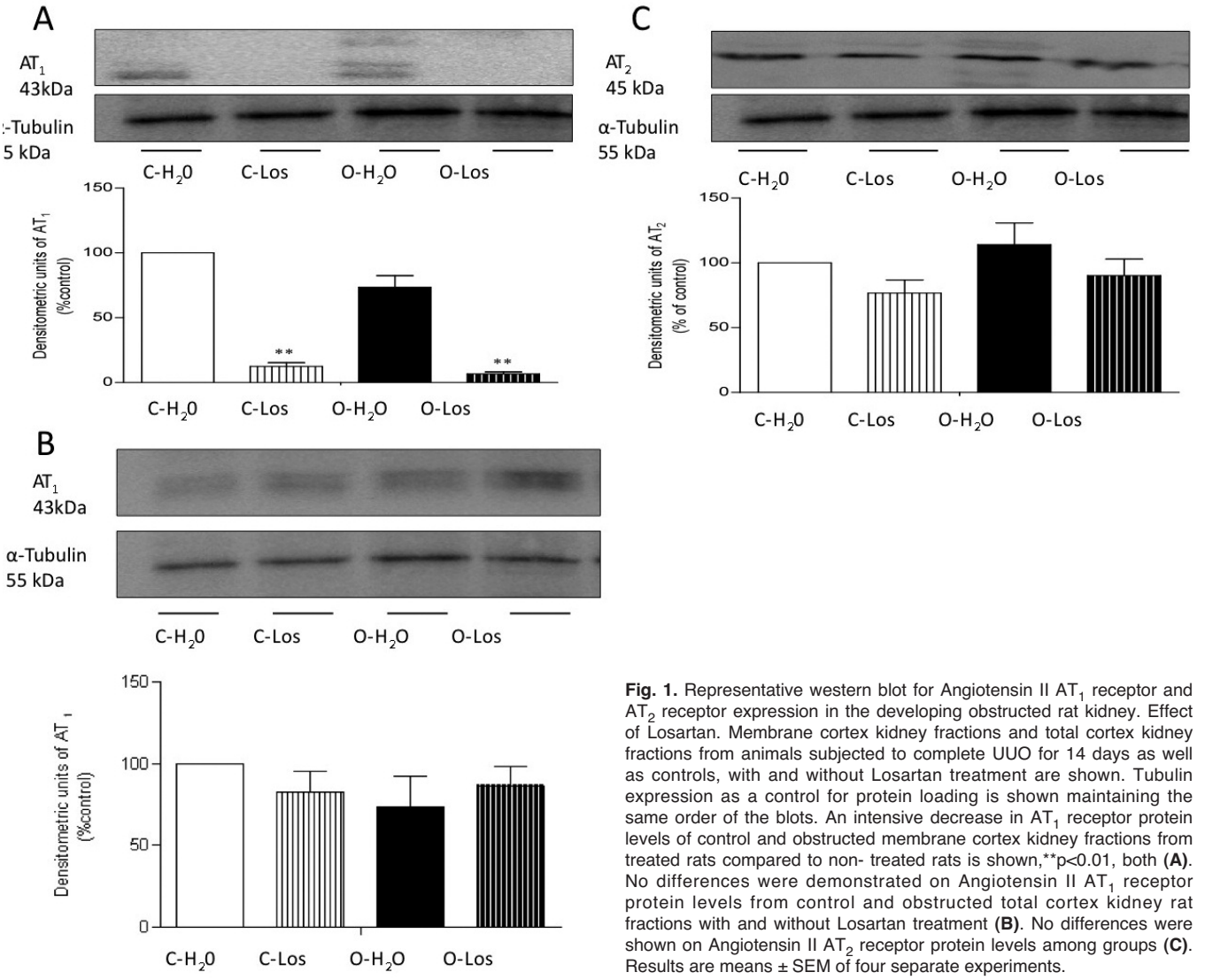

Fig. 1. Representative western blot for Angiotensin II AT_1 receptor and AT_2 receptor expression in the developing obstructed rat kidney. Effect of Losartan. Membrane cortex kidney fractions and total cortex kidney fractions from animals subjected to complete UUO for 14 days as well as controls, with and without Losartan treatment are shown. Tubulin expression as a control for protein loading is shown maintaining the same order of the blots. An intensive decrease in AT_1 receptor protein levels of control and obstructed membrane cortex kidney fractions from treated rats compared to non- treated rats is shown,**p<0.01, both **(A)**. No differences were demonstrated on Angiotensin II AT_1 receptor protein levels from control and obstructed total cortex kidney rat fractions with and without Losartan treatment **(B)**. No differences were shown on Angiotensin II AT_2 receptor protein levels among groups **(C)**. Results are means ± SEM of four separate experiments.

differences among groups in terms of AT_1 receptor expression (Fig. 1B). No differences were observed in AT_2 receptor protein expressions before and after AT_1 receptor inhibition in 14 day obstructed membrane cortex kidney fractions (Fig. 1C).

Renal tubular cell apoptosis induction in obstruction

Histochemistry. Tunel Assay

Transverse renal cortex sections from 14 day rat

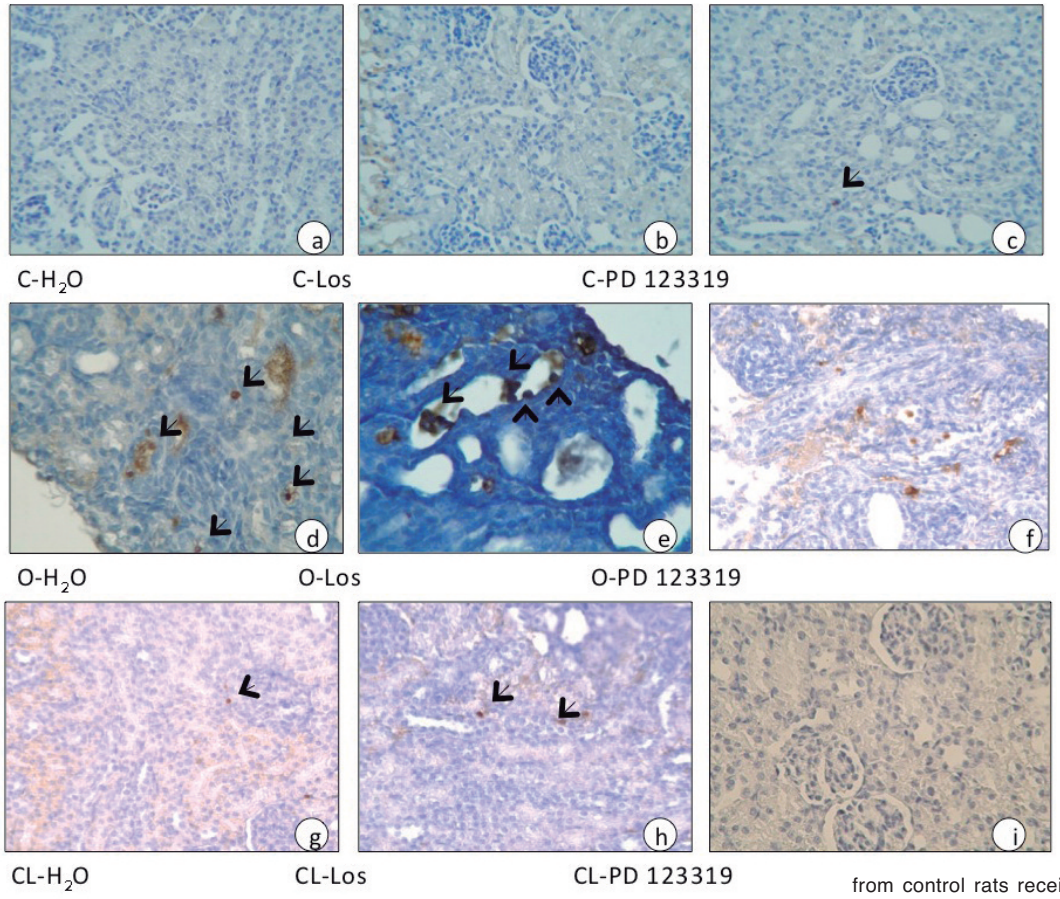

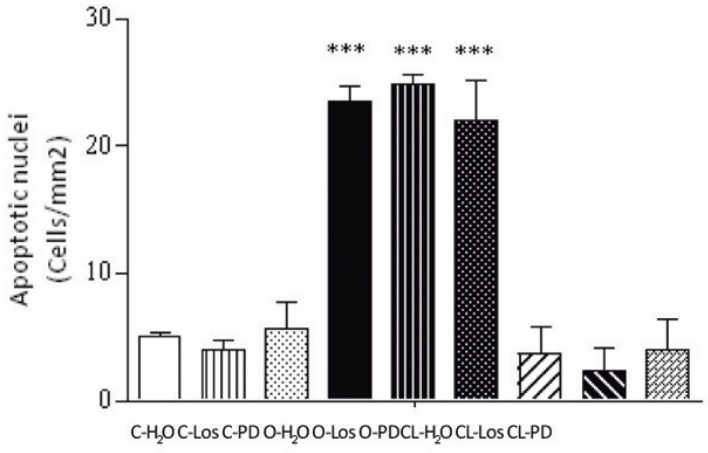

Fig. 2. Representative photomicrographs of renal sections from control, obstructed and contralateral cortexes vehicle-treated, Losartan-treated and PD-123319 treated rats. Brown-staining apoptotic nuclei were identified by TUNEL technique and quantified in cross sectioned cortex areas. **a, b and c.** Cortex kidney sections from control rats receiving vehicle, Losartan or PD-123319 treatment respectively. Apoptotic cells are rarely seen in epithelial cells from CCD and PT. **d, e, and f.** Obstructed cortex kidney sections from UUO rats receiving vehicle, Losartan or PD-123319 treatment. Apoptotic nuclei appear as heavy brown-staining nuclei in dilated collecting ducts and in lesser proportion in proximal tubules. Increased number of TUNEL-positive tubular epithelial cells in cortex from obstructed non treated animals ($O\text{-}H_2O$) compared to control ($C\text{-}H_2O$), ***$p<0.001$. Moreover, in obstructed cortex from Losartan-treated animals (O-Los), and PD123319 treated animals the number of TUNEL-positive apoptotic cells was significantly higher than in the control animals, ***$p<0.001$. **g, h and i.** Contralateral cortex kidney sections from UUO rat receiving vehicle, Losartan or PD-123319 treatment. No significant differences were found in contralateral cortex kidney sections among groups. Each bar represents the mean±S.E.M. of 2 separate experiments. x 400

obstructed kidneys and the corresponding control and contralateral kidney cortex sections were stained for the presence of apoptotic nuclei by the terminal deoxynucleotidyl transferase mediated dUTP nick-end labelling technique after saline, Losartan or PD-123319 treatments. As shown in Figure 2, dilated cortical tubules and less proximal tubules from cortex of obstructed neonatal kidney rats after 14 days contained relatively high numbers of apoptotic nuclei characterized by brown nuclear staining, corresponding to fragmented nuclear chromatin (Fig. 2d). In contrast, apoptotic nuclei were rarely seen in control or contralateral cortex kidneys (Fig. 2a,g). The administration of Losartan had no effect on the development of apoptosis in UUO (Fig. 2e), or in contralateral and control kidneys (Fig. 2b,h).

Moreover, tubular cell apoptosis of control kidneys was 5 fold less than that measured in the obstructed kidney after 14 days of UUO with and without Losartan treatment (C+H_2O:5±0.4vs O-H_2O: 23.5±1.2, vs O-Los 24.8±0.8).

Apoptotic cell response was also shown in 14 day obstructed kidney cortex rats after treatment with PD-123319 (Fig. 2f), demonstrating absence of a cytoprotective role of the selective AT_2 receptor

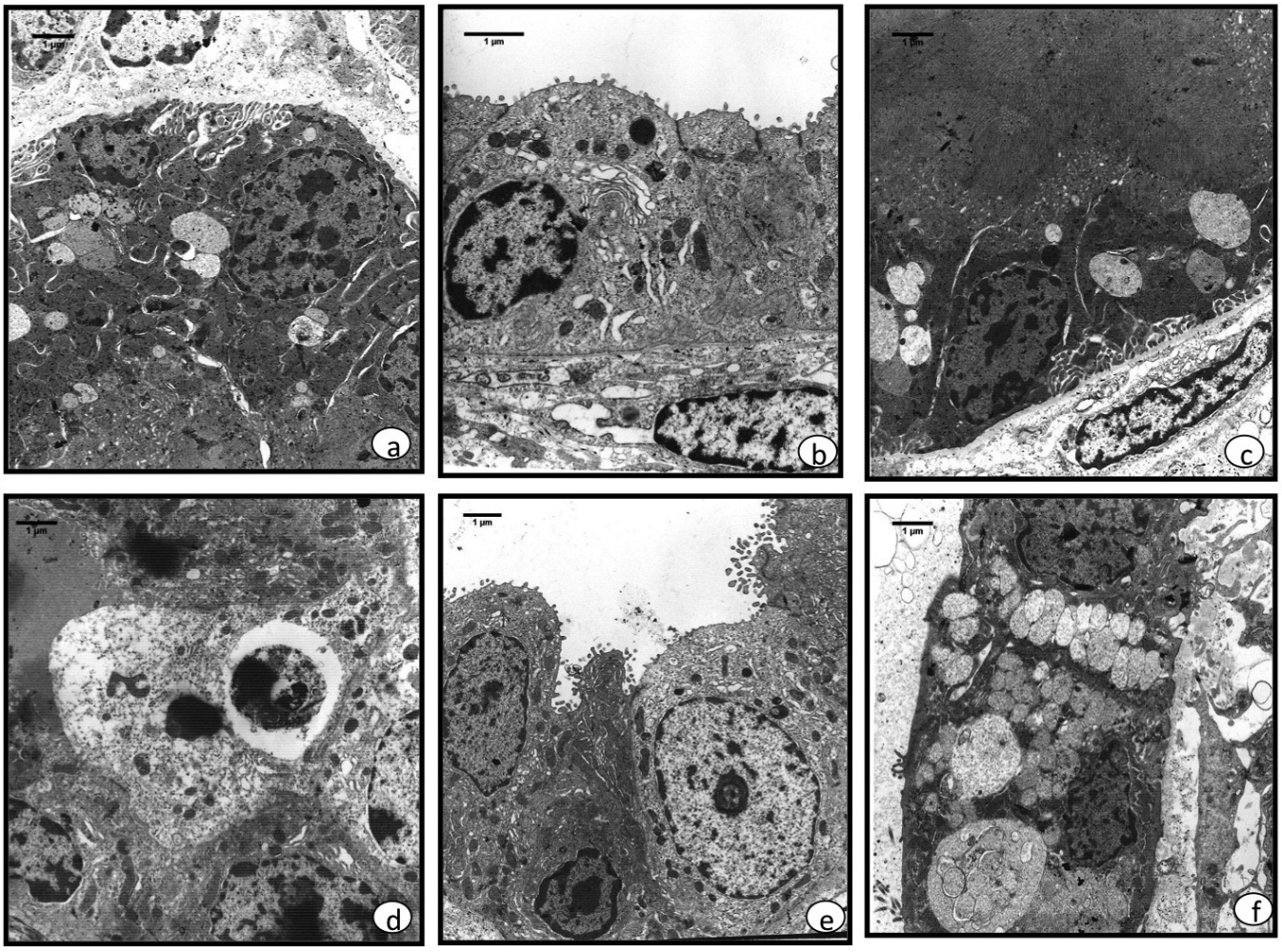

Fig. 3. Transmission electron micrograph of cortex sections from control and obstructed kidneys. Cortex sections from control kidney. Proximal tubule from control cortex kidney with dense population of apical microvilli at the brush border membrane, interdigitated ephitelium and numerous mitochondria **(a)**. Cortical collecting duct cell from Losartan treatment control cortex kidney rats were showed short apical microvilli and few mitochondria **(b)**. The proximal tubule epithelial cells also showed some endocityc vacuoles normally present in proximal tubule segment **(c)**. Ultrastuctural examination confirmed the presence of apoptotic cells in obstructed cortex kidney rats. In 14-day obstructed kidney a phagocytose apoptotic body was found in proximal tubule cell cytoplasm **(d)**. Fig 3e showed an apoptotic cell with condensed nuclear chromathin and cytoplasmic shrinkage in 14 day Losartan obstructed cortex kidney **(e)**. In CCD Losartan treatment cortex kidney 2 types of intracellular vacuoles were found; one of them, small vacuoles with electron- dense material, the second, bigger vacuoles with electron-lucent material. a, b, x 4,000; c x 7,000; d, e, x 4,400; f, x 3,000

inhibitor. The AT_2 receptor inhibition had no effect on kidney from control or from contralateral kidney after 14 days of obstruction (Fig. 2c and i respectively).

Five fold higher apoptotic cells were shown in CD from 14 day obstructed kidney after AT_2 receptor inhibitor related to that measured in controls:O-PD123319: 22.0±3.15 vs C-PD 123319: 5.7±2.1 , ***p<0.001n=2.

Ultrastructural findings in neonatal obstructive nephropathy. Transmission electron microscopy

To further confirm the presence of apoptotic induction, we examined the ultrastuctural morphology in 14 day-obstructed and control cortex kidney with and without Losartan treatment, using transmission electron microscopy.

After 14 day Losartan treatment, a typical apoptotic cell with cellular shrinkage and condensed nuclear chromatin was found in CCD cells from neonatal rats subjected to ureteral obstruction (Fig. 3e).Illustration 3f shows a CCD cell from 14-day Losartan treatment rat with numerous cytoplasmic vacuoles, although the number, arrangement and electron density were not consistent with those apical vacuoles that were normally seen in control cortex kidney.

On the contrary, control cortex kidney showed a well preserved structure with a dense population of apical microvillae, a great number of mitochondria and some normal endocityc vacuoles were found in proximal tubule epithelial cell from sham operated cortex kidney rats, Fig. 3a,c.

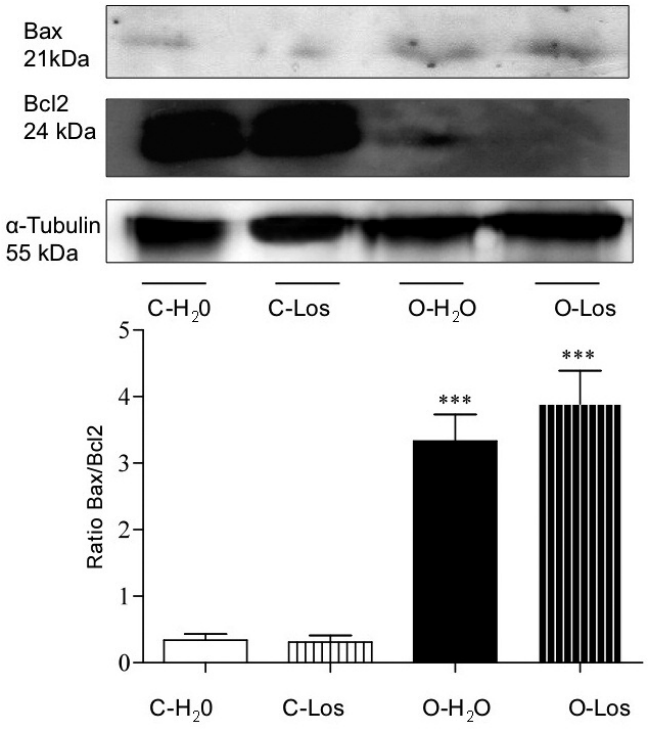

Fig. 4. Losartan effect on mitochondrial apoptotis during neonatal UUO. Bax/BcL-2 protein expression. Representative western blot and densitometric analysis for protein levels of BcL-2 and Bax as a proapoptotic ratio from 14 day obstructed- cortex kidneys after Losartan treatment. The relative amount of BcL-2 and Bax protein levels were determined after normalization of the level of BcL-2 and Bax protein of the appropriate control. Increased in Bax / BcL-2 ratio from obstructed kidney cortex after Losartan and vehicle treatment compared to controls, ***p<0.001, both. Data represent the means ± SEM of five independent experiments.

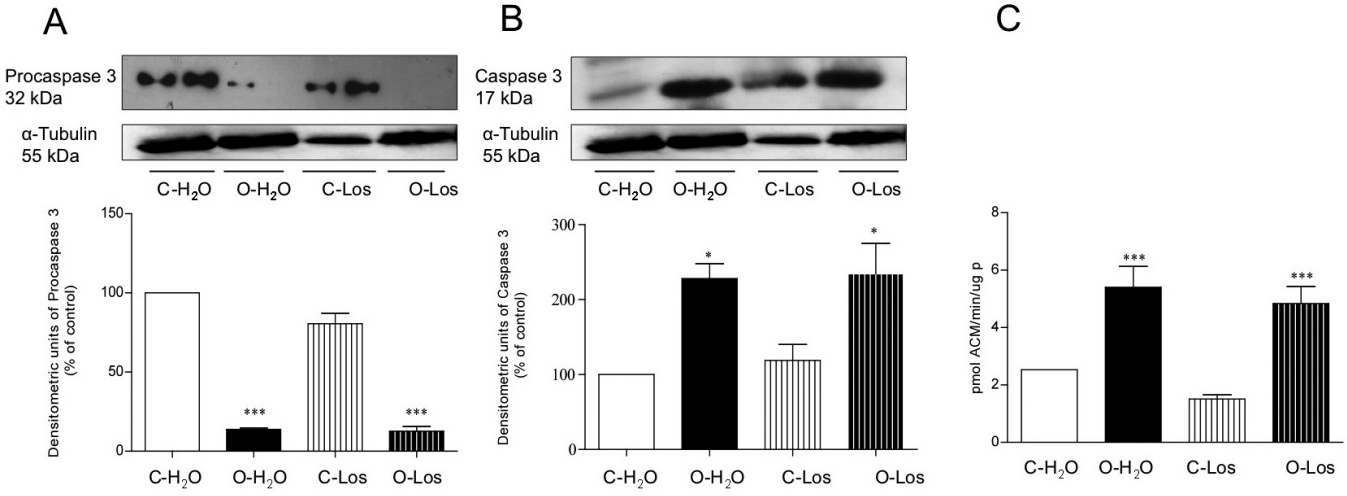

Fig. 5. Mitochondrial apoptotic pathway induction in Losartan- treated obstructed rats. Renal Procaspase and caspase 3 expression and activity. Western blot analysis for 32 kDa pro-caspase 3 **(A)**, caspase 3 protein **(B)** and caspase 3 activity **(C)** in kidney cortex from Losartan-treated and vehicle -treated UUO rats. Representative western blot analysis for 32 kDa pro-caspase 3 protein in control cortex from rats without and with Losartan treatment (C-H_2O and C-Los) and in obstructed cortex without and with Losartan treatment (O-H_2O and O-Los). Densitometric analysis of procaspase 3 protein showed decreased protein level in 14 day O-H_2O and O-Los vs C-H2O ***p<0.001 both, n=4. Increased caspase 3 protein abundance after Losartan and vehicle treatment in obstruction vs controls; *p<0.05 both, n=4. Caspase 3 activity was assessed by level of Ac-DEVD-AMC cleavage release of fluorescence AMC tag. Activity was expressed as pmol AMC/min/μg protein. Increased caspase 3 activity was demonstrated in UUO cortex after Losartan and vehicle treatment vs control ***p<0.001, both n=4. Pro-caspase 3 protein , caspase 3 protein and caspase 3 activity assay data were obtained from the same four independent samples.

The proapoptotic regulation of the BcL-2 family proteins after AT_1 receptor inhibition in neonatal UUO

Anti-apoptotic BcL-2 protein expression was significantly decreased after 14 days of obstruction related to control 25.23±3.23 p<0.01; 27.48±2.7, p<0.01 respectively. These changes resulted in a 3 fold increase in pro-apoptotic ratio Bax/BcL-2 in obstructed kidneys, which reflects a change in the balance between cell life and death-promoting BcL-2/Bax protein levels. Lack of

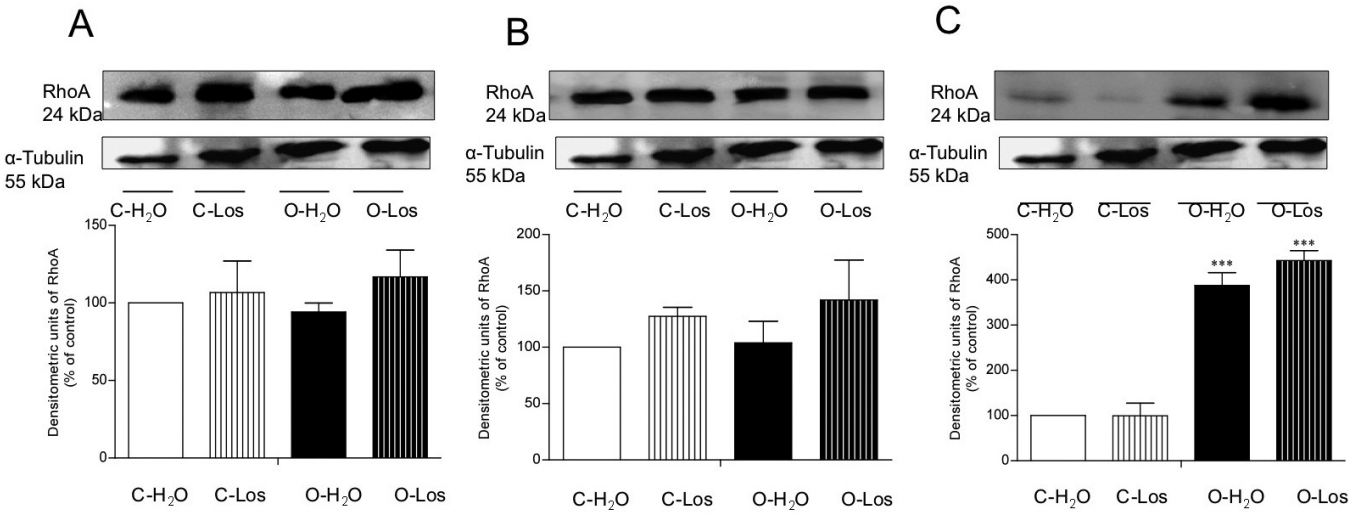

Fig. 6. Rho A activation in obstruction after AT_1 receptor inhibition. Semiquantitative immunoblotting of total **(A)**, cytosol **(B)** and membrane **(C)** fractions of cortex from obstructed and control rats with and without Losartan treatment. Immunoblots reacted with anti Rho A antibody and revealed a single 24 kDa band. The intensity of the bands was quantified by densitometry and was expressed as arbitrary units. Higher expression of membrane-bound Rho A (active form) was shown in O-Los vs control, **p<0.01 and in O-H_2O vs control ** p<0.01.

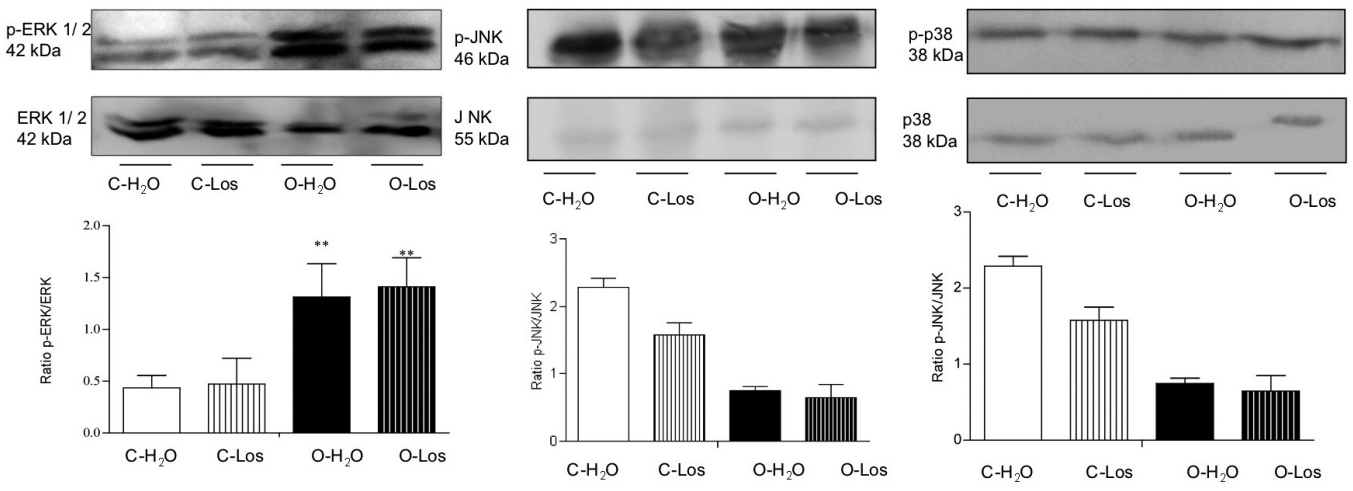

Fig. 7. Effect of AT_1 receptor inhibition on ERK1/2 activity in obstructed membrane cortex. **A.** Corresponds to ERK1/2 activity was assessed by western blotting using phospho-ERK1/2 and non-phospho- ERK1/2 (total) antibodies and quantified by densitometric scanning. The upper panel was probed with an antibody recognizing the phosphorylated (activated) form of ERK-1/2. The lower panel shows the blot reprobed with an antibody recognizing the nonphosphorylated form (i.e., total) ERK-1/2. Densitometric analysis presented as the ratio of activated ERK to total ERK (pERK/ERK). ** p<0.01 indicates that the value is significantly different from control. Data are mean ± SEM of 5 experiments. JNK and p38 MAPK phosphorylation profiles after AT_1 receptor inhibition treatment are shown in **B** and **C** respectively. Cortex kidney from control and obstructed rats with and without Losartan treatment were subjected to western blotting with anti- phospho-JNK and non phospho-JNK(total) and p38 anti-phospho-Thr 180/Tyr 182 p38 antibodies and quantified by densitometric scanning. The upper panel was probed with an antibody recognizing the phosphorylated (activated) form of the antibody. The lower panel shows the blot reprobed with an antibody recognizing the nonphosphorylated form (i.e., total). A significant decrease of JNK phosphorylation protein levels were shown in obstructed cortex kidney wihout and with Losartan treatment **(B)**. Densitometric analysis showed no differences for p38 kinase among groups n:4 **(C)**.

AT_1 receptor inhibition effect was demonstrated in the obstructed kidney, by the increased apoptotic response through the mitochondrial pathway with BcL-2 downregulation and increased pro-apoptotic ratio Bax/BcL-2 (Fig. 4).

Non significant differences in the pro-apoptotic ratio Bax/BcL-2 expression were shown in control kidneys with and without Losartan treatment (Fig. 4).

Caspase 3 expression and activity in obstruction induced- apoptosis. Effect of Losartan

Pro-caspase, caspase 3 protein levels and caspase 3 activity were measured to determine if mechanical obstruction induced apoptosis in epithelial tubule cells occurred via the caspase cascade, which is the central protease in the cell death pathway.

Western blot analysis demonstrated an intensive decrease in 32 kDa procaspase 3 protein expression due to its cleavage to an active protein, as determined by an increase in caspase 3 protein abundance and enhanced caspase 3 activity in response to obstruction for 14 days with and without Losartan treatment (Fig. 5A-C, respectively). Conversely, no differences were shown in procaspase and caspase 3 protein levels or in caspase 3 activity, in control cortex with and without Losartan treatment for 14 days (Fig. 5A-C).

RhoA activation in obstruction-induced apoptosis. Effect of AT_1 receptor inhibition

RhoA activation as a result of the stretch insult by obstruction could represent a significant step. Membrane-bound RhoA activation is involved in the regulation of cellular processes, such as organization of the microfilamental network, cell-cell contact and apoptosis. To address the question of whether RhoA protein is involved in obstruction tubular cell apoptotic response regulation we next analyzed the expression of activated membrane-bound Rho A expression by western blotting. As shown in Figure 6, we found that membrane associated Rho A was increased two fold in the obstructed kidney rats ($p<0.01$). The absence of Losartan effect was demonstrated through the overexpression of membrane Rho A in 14 day obstructed- treated cortex kidney rats.

Obstruction induced apoptosis stimulated ERK1/2 expression. Effect of AT_1 receptor inhibition

Then, we tested the hypothesis of MAPK activity involvement in obstruction-induced apoptosis. We further investigated the contributions to cell death of mitogen-activated protein (MAP) kinase family members, including ERK (extracellular signal-regulated kinase), JNK (c-JNK NH2-terminal protein kinase), and p38, before and after AT_1 receptor inhibition.

Increased induction of ERK1/2 phosphorylation, normalized to the total ERK1/2 level, was shown in 14 day obstructed membrane cortex. No significant effect of AT_1 receptor inhibition was demonstrated in obstructed kidney rats, with increased ERK phosphorylation levels above those seen in controls (Fig. 7A). Concurrent inhibition of JNK for apoptosis induction was demonstrated in obstructed cortex kidneys pretreated or not with Losartan. (Fig. 7B). Conversely, it was not noted that p38 MAPK played a role in the obstruction-induced apoptosis in obstruction (Fig. 7C). Our results indicate that apoptosis in obstructed cortex tubular cells was regulated by the opposing actions of the ERK and c-JNK with p38 MAP kinase pathways.

Discussion

The RAS plays a central role, not only in the progression of renal disorders, but also in normal renal development and maturation. In support of this notion, pharmacological interruption of Angiotensin II type-1 (AT_1) receptor leads to a broad spectrum of renal maldevelopment, including thickened vasculature, abnormal glomeruli, tubular dilatation, and increased accumulation of extracellular matrix in animals with ongoing nephrogenesis (Friberg et al., 1994; Chevalier et al., 1999, 2002).

Modulation of renal apoptosis by Angiotensin II is complex and dependent on the stage of renal maturation and the timing and severity of renal injury due to urinary obstruction.

Here, we have demonstrated the convergence of at least two independent signal pathways, ERK MAP kinase and the Rho A, a small GTPase are required for the induction of the mitocondrial apoptotic response in renal tubular cells from the 14 day obstructed kidneys. Selective AT_1-receptor inhibition during the postnatal renal maturation had no effect on the renal cellular response in the kidney subjected to UUO for 14 days or in the contralateral and control kidney.

In the experimental model of complete unilateral ureteral obstruction with increased intrarenal Angiotensin II we have shown the decrease on AT_1 receptor protein expression in cortex membrane fraction following AT_1 inhibition for 14 days. However, there were no differences demonstrated on the AT_1 receptor at protein levels in total cortex kidney fractions after Losartan administration among the groups.

The cortex tubular epithelial cells displayed an apoptotic response with a 5 fold increase in apoptotic nuclei, characterized by apoptotic bodies or condensed nuclear chromatin after AT_1 Angiotensin II receptor inhibition. Likewise, ultrastructural findings in obstructed PT cells showed reduction in mitochondria number and microvillus appeared dispersed and decreased in number. Typical morphological features of apoptotic cells, including chromatin condensation in dense masses under the nuclear membrane, compaction of the cytoplasm, crowding of organelles and surface protuberances were demonstrated.

In regard to the study sequence the presence of AT_2 Angiotensin II receptor expression was demonstrated on day 14 of obstruction by western blot analysis. AT_2

receptor has been shown to be mainly expressed in fetal tissues (Ciuffo et al., 1993) and neonatal kidneys (Stoll et al., 1995), decreasing after birth, which implies that the AT_2 receptor might have a role during kidney organogenesis. It has been reported that in vivo exogenous Angiotensin II increases renal apoptosis after a 3 day period of complete UUO in the neonatal rat, an effect suppressed by AT_2-receptor inhibition (Chevalier et al., 1999). Nevertheless, in this model of neonatal rat kidney obstructed for 14 days, the response to the selective Angiotensin AT_2-receptor inhibition showed no effect on cellular tubular apoptosis response. Similar to our data, AT_2-receptor activity inhibition in rat partial UUO, from day 10 to day 20, did not confer protection from obstruction-induced apoptosis (Coleman et al., 2007). Unopposed stimulation of AT_2 receptors has been suggested to be involved in Losartan apoptosis induction (Bonnet et al., 2002). However, non increased AT_2 protein expression was demonstrated in our study. The persistence of apoptotic response after Losartan in 14 day obstructed kidney was shown to be associated with the mitochondrial signaling pathway through the increased proapoptotic ratio Bax/BcL-2 and, consequently increased caspase activity and expression. For these results, the absence of the Losartan effect was shown in 14 day obstructed kidney tubular cells.

In view of the likely role of apoptosis in contributing to tubular atrophy in the obstructed kidney, attention was turned to the signaling pathways involved in the regulation of the apoptotic response. In this study, we examined a less well-characterized RhoA function; the one in cell survival. RhoA, a founding member of the small Rho GTPase family, is known to control epithelial morphogenesis and integrity through its ability to regulate the cytoskeleton, inducing the formation of stress fibres, membrane ruffing and focal adhesion (Ridley et al., 1992). Regulation of cell cytoskeleton may be important for functions such as apoptosis (Rouslahti and Reed, 1994), where cell adhesion may play a critical role (Nobes and Hall, 1995). Based on our observations, we have shown the RhoA pathway involvement through its translocation and further membrane-associated GTP -bound activation on apoptosis induction regulation in obstructed kidney tubular cells from non treated and Losartan treated animals.

In this regard, it has previously been reported that several human Rho proteins, including Rho A and Rho C, are capable of inducing apoptosis in different cell systems like murine NIH3T3 fibroblasts and they are drastically inhibited by ectopic expression of Bcl2, both under *in vitro* and *in vivo* conditions (Esteve et al., 1998).

We also demonstrated the contribution of signaling cascades mediating ERK1/2 MAPK activation, to morphological changes that are characteristic of apoptosis. While increased ERK1/2 phosphorylation and activation was demonstrated, JNK MAP kinases activation was seen to be abolished on obstruction-induced apoptosis. The absence of the p38 MAPK signaling pathway activation was shown after obstruction.

Furthermore, the apoptotic response was demonstrated to be regulated by the opposing actions of the ERK and JNK-p38 MAP kinase signaling pathways in obstructed renal tubular cells, with an absence of effect after Losartan treatment.

Although the ERK, JNK and p38 MAP kinases are related structurally and are activated by similar kinase cascades, they are activated by different extracellular stimuli (Davis, 1994). These differences in the response to extracellular stimuli and in substrate specificity may explain our results, which reveal that only ERK MAP kinase was activated, promoting programmed cell death. Similar to our results, it is known that ERK activation occurs both in vitro mechanical stretch of tubular cells and in vivo following UUO, in which ERK activation is maximal in the most dilated (most stretched) sections of the tubule (Kushida, 2001; Alexander et al., 2004).

Angiotensin has been linked to cyclic stretch induced MAPK activation (Komuro et al., 1996; Kudoh et al, 1998). Moreover, Angiotensin II activates signaling molecules, including small G-proteins through AT_1 receptor (Hall, 1998). Nevertheless, our results showed no effect on Angiotensin type 1 AT_1 inhibition in obstruction. Rho A GTPase activation associated with increased pERK1/2, as events involved in tubular cell apoptosis regulation, were demonstrated after Losartan administration.

Lack of resistance to obstruction-induced cell death by Angiotensin type 1 AT_1 (Losartan) receptor antagonist, allow us to suggest the important role of mechanical stretch in 14 day obstructed tubular cells.

With respect to this, we have previously provided evidence demonstrating that obstruction- induced renal tubular cell apoptosis was associated with target downregulation of NHE1 protein expression, a plasma membrane Na^+/H^+ antiporter typically associated with maintenance of intracellular volume and pH (Komuro et al., 1998, Manucha et al., 2007).

In conclusion, this study provides data supporting the hypothesis that AT_1 receptor inhibition has no effect on tubular cell mitochondrial apoptosis induction regulated by RhoA activation and pERK stimulation signaling pathways in neonatal UUO for 14 days.

Additional studies will be required to evaluate the temporal switch from an injurious to a cytoprotectice effect of Angiotensin II inhibition on neonatal obstructive nephropathy.

Acknowledgements. This work was performed with financial support from CONICET, PICT/2005 N 33827 and from the Research and Technology Council of Cuyo University (CIUNC) Mendoza, Argentina / N: 1143 / 06 to P. G. Vallés. Portions of this study were presented as an abstract form at the Latinoamerican Congress of Pediatric Nephrology in Buenos Aires, Argentina, October , 2008.

References

Alenghat F.J. and Ingber D.E. (2002). Mechanotransduction:all signals point to cytoskeleton, matrix, and integrins. Sci. STKE, PE6.

Alexander D., Alagarsamy S. and Douglas J.G. (2004). Cyclic stretch induced cPLA2 mediates ERK 1/2 signaling in rabbit proximal tubule cells. Kidney Int. 65, 551-563.

Beharrie A., Franc-Guimond J., Rodriguez M.M, Au J, Zilleruelo G, Abitbol CL. (2004). A functional immature model of chronic partial ureteral obstruction. Kidney Int., 65, 1155-1161.

Bonnet F., Candido R., Carey R.M., Casley D., Russo L.M., Osicka T.M., Cooper M.E. and Cao Z. (2002). Renal expression of angiotensin receptors in long-term diabetes and the effects of angiotensin type 1 receptor blockade. J. Hypertens. 20, 1615-1624.

Cachat F, Lange-Sperandio B, Chang A.Y, Kiley S.C, Thornhill B.A, Forbes M.S. and Chevalier R.L. (2003). Ureteral obstruction in neonatal mice elicits segment-specific tubular cell responses leading to nephron loss. Kidney Int., 63, 564-575.

Chen C.O., Park M.H., Forbes M.S., Thornhill B.A., Kiley S.C. and Chevalier R.L. (2007). Angiotensin converting enzyme inhibition agravates renal interstitial injury resulting from partial unilateral ureteral obstruction in the neonatal rat. Am. J. Physiol. Renal. Physiol. 292, F946-F955.

Chevalier R.L. (1996). Growth factors and apoptosis in neonatal ureteral obstruction. J. Am. Soc. Nephrol. 7, 1098- 1105.

Chevalier R.L. (2003). Ureteral obstruction in neonatal mice elicits segment-specific tubular cell responses leading to nephron loss. Kidney Int. 63, 564-575.

Chevalier R.L. and Cachat F. (2001). Role of Angiotensin II in chronic ureteral obstruction. In: The renin-angiotensin system and progression of renal diseases. Wolf G. (ed). Karger, Basel. pp 250-260.

Chevalier R.L., Kim A., Thornhill B.A. and Wolstenholme J.T. (1999). Recovery following relief of unilateral ureteral obstruction in the neonatal rat. Kidney Int., 55, 793-807.

Chevalier R.L, Thornhill B.A. and Wolstenholme J.T. (1999). Renal cellular response to ureteral obstruction: role of maturation and Angiotensin II. Am. J. Physiol. Renal. Physiol. 277, F41-F47.

Chevalier R.L., Thornhill B.A., Chang A.Y., Cachat F. and Lackey A. (2002). Recovery from release of ureteral obstruction in the rat: relationship to nephrogenesis. Kidney Int. 61, 2033-2043.

Ciuffo G.M., Viswanathan M., Seltzer A.M., Tsutsumi K. and Saavedra J.M. (1993). Glomerular Angiotensin II receptor subtypes during development of rat kidney. Am. J. Physiol. 265, F264-F271.

Coleman C.M., Minor J.J., Burt L.E., Thornhill B.A., Forbes M.A. and Chevalier R.L. (2007). Angiotensin AT_1-receptor inhibition exacerbates renal injury resulting from partial unilateral ureteral obstruction in the neonatal rat.Am. J. Physiol. Renal Physiol. 293, F262-F268.

Esteve P., Embade N., Perona R., Jimenez B., Del Peso L., Arends M., Miki T. and Lacal J.C. (1998). Rho-regulated signals induce apoptosis in vitro and in vivo by a p53-independent, but Bcl2 dependent pathway. Oncogene 17, 1855 -1869.

Friberg P., Sundelin B., Boman S.O., Bobik A., Nilsson H., Wickman A., Gustaffson H., Petersen J. and Adams M.A. (1994). Renin-Angiotensin system in neonatal rats induction of renal abnormality in response to ACE inhibition or Angiotensin II antagonism. Kidney Int. 45, 485-492.

Galbraith C.G., Yamada K.M. and Sheetz M.P. (2002). The relationship between force and focal complex development. J. Cell Biol. 159, 695-705.

Guron G. and Friberg P. (2000). An intact renin-Angiotensin system is a prerequisite for normal renal development. J. Hypertens. 18, 123-137.

Hall A. (1998). Rho GTPases and the actin cytoskeleton. Science 279, 509-514.

Ionin B., Hammamieh R., Shupp J.W., Das R., Pontzer C.H. and Jett M. (2008). Staphylococcal enterotoxin B causes differential expression of Rnd3 and RhoA in renal proximal tubule epithelial cells while inducing actin stress fiber assembly and apoptosis. Microbial Pathogenesis 45, 303-309.

Kohaut E.C. and Tejani A. (1996). The 1994 annual report of the North American Pediatric Renal Transplant Cooperative Study. Pediatr Nephrol. 10, 422 434.

Komuro I., Kudo S. and Yamazaki T., Zou I., Shiojima I. and Yazaki Y. (1996). Mechanical stretch activates the stress-activated protein kinases in cardiac myocytes. FASEB. J. 10, 631-636.

Kudoh S., Komuro I., Hiroi Y., Zou Y., Harada K., Sugaya T., Takekoshi N., Murakami K., Kadowaki T. and Yazaki Y. (1998). Mechanical stretch induces hypertrophic responses in cardiac myocytes of Angiotensin II type 1a receptor knockout mice. J. Biol. Chem. 273, 24037-24043.

Kushida N., Kabuyama Y., Yamaguchi O. and Homma Y. (2001). Essential role for extracellular Ca^{2+} in JNK activation by mechanical stretch in bladder smooth muscle cells. Am. J Physiol. Cell Physiol. 281, C1165-C1172.

Manucha W., Carrizo L., Ruete C. and Vallés PG. (2007). Apoptosis induction is associated with decreased NHE1 expression in neonatal ureteral obstruction. B. J. Urol. 100, 191-198.

Manucha W., Oliveros L, Carrizo L., Seltzer A. and Vallés P. (2004). Unilateral Ureteral Obstruction: Losartan modulation on NOS isoforms and COX-2 expression in early renal fibrogenesis Kidney Int. 65, 1-17.

Nguyen H.T., Hsieh M.H., Gaborro A., Tinloy B., Phillips C. and Adam R.M. (2006). JNK/SAPK and p38 SAPK-2 mediate mechanical stretch-induced apoptosis via caspase-3 and -9 in NRK-52E renal epithelial cells. Nephron Exp. Nephrol. 102, e49-e61.

Nobes C.D and Hall A. (1995). Rho, rac, and cdc42 GTPases regulate the assembly of multimolecular focal complexes associated with actin stress fibers, lamellipodia, and filopodia. Cell, 81, 53-62.

Ohtsu H., Suzuki H., Nakashima H., Dhobale S., Frank G.D., Motley E.D. and Eguchi S. (2006). Angiotensin II signal transduction through small GTP-binding proteins: mechanism and significance in vascular smooth muscle cells. Hypertension. 48, 534-540.

Peters C.A. (1995). Urinary tract obstruction in children. J. Urol. 154, 1874 1883.

Davis R.J. (1994). MAPKs: new JNK expands the group. Trends Biochem. Sci. 19, 470.

Ridley A.J., Paterson H.F., Johnston C.L., Diekmann D. and Hall A. (1992). The small GTP-binding protein rac regulates growth factor-induced membrane ruffling. Cell 70, 389 -399.

Riveline D., Zamir E., Balaban N.Q., Schwarz U.S., Ishizaki T., Narumiya S., Kam Z., Geiger B. and Bershadsky A.D. (2001). Focal contacts as mechanosensors: externally applied local mechanical force induces growth of focal contacts by an mDia1-dependent and ROCK-independent mechanism. J. Cell Biol. 53, 1175-1186.

Rouslahti E. and Reed J.C. (1994). Anchorage dependence, integrins,

and apoptosis. Cell 77, 477-478

Stoll M., Steckelings U.M., Paul M., Bottari S.P, Metzger R. and Unger T. (1995). The angiotensin AT_2-receptor mediates inhibition of cell proliferation in coronary endothelial cells. J. Clin. Invest. 95, 651-657.

Tian W., Zhang Z. and Cohen D.M. (2000). MAPK signaling and the kidney. Am. J. Physiol. Renal Physiol. 279, F593-F604.

Topcu S.O., Pedersen M., Nørregaard R., Wang G., Knepper M., Djurhuus J.C., Nielsen S., Jørgensen T.M. and Frøkiaer J. (2007). Candesartan prevents long-term impairment of renal function in response to neonatal partial unilateral ureteral obstruction. Am. J. Physiol. Renal Physiol. 292: F736-F748.

Yoo K.H, Thornhill B.A. and Chevalier R.L. (2000). Angiotensin stimulates TGF-beta 1 and clusterin in the hydronephrotic neonatal rat kidney. Am. J Physiol. Regul. Integr. Comp. Physiol. 278, R640-R645.

Accepted February 8, 2012